Chemical Science Review and Letters ISSN 2278-6783

Research Article

Corrosion Inhibition of Mild steel in 1M HCl in the Presence of *Spathodea campanulata* Leaves and Flowers

Prithiba A* and Rajalakshmi R

Department of Chemistry, Avinashilingam Institute for Home Science and Higher Education for Women, Coimbatore India

Abstract

Plant parts of ***Spathodea campanulata*** (Leaves and flowers) were tried as prospective inhibitors for the corrosion of mild steel in the presence of in1 M HCl by means of potentiodynamic polarization, electrochemical impedance spectroscopic and mass loss techniques. Results obtained reveal that the leaves and flowers extract of ***Spathodea campanulata*** act as an effective inhibitor for mild steel in the examined acidic medium. Inhibition efficiency was found to be influenced by concentration of the inhibitor, impact of immersion time and temperature.The inhibitive effect could be attributed to the phytochemical constituents present in the inhibitor. The adsorption characteristics of the inhibitor were approximated by Langmuir adsorption isotherm. Thermodynamic parameters reflect that the adsorption process was spontaneous. Polarisation curves indicated that the inhibitors acted through mixed mode of inhibition. The results obtained from various methods employed were in good agreement. Surface morphology was carried out to ascertain the inhibitive nature of the studied inhibitor.

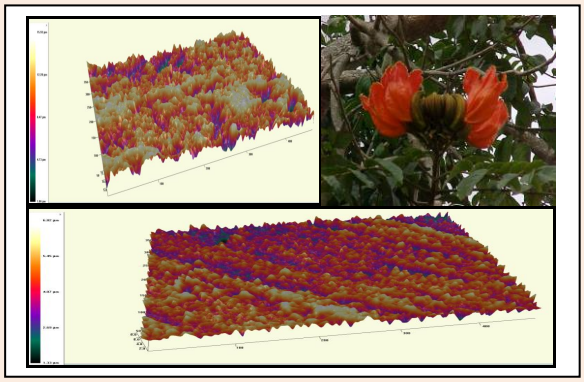

Keywords: Corrosion, inhibitor, *Spathodea*, Mass loss, *campanulata* leaves, flower, Electrochemical techniques, SEM-EDAX

***Correspondence**
Prithiba. A
Email: prithipete@gmail.com

Introduction

Rapid technological development has necessitated the increasing use of mild steel in various industries due to its low cost and easy availability. Mineral acids namely hydrochloric and sulphuric acid are most commonly used for various purposes namely acid pickling , acid descaling and oil well acidizing .The aggressive nature of these acids induce corrosive attack on the metal surface that can be controlled by the application of inhibitors. Corrosion is the damage of material resulting from exposure and interaction with the environment. It is a major problem that must be confronted for safety, environment and economic reasons[1,2]. Many synthetic organic compounds are effective in minimising metal loss but their toxicity and environmental issues have prompted researchers to explore the ecofriendly option of utilising natural products as corrosion inhibitors. Numerous naturally occurring substances have been documented as inhibitors[3]. Sprouted seeds of *Phaseolus aureus* [4] *Cyamopsis* tetragonaloba [5], *Ervatamia coronaria* [6], *Cocos nucifera* [7], are some of the investigated inhibitors of our research team. *Spathodea campanulata* belongs to the family Bignoniaceae and is one of the most invasive species with high medicinal value. The present research work aims at assessing the effectiveness of *Spathodea campanulata* leaves [8] and flowers extracts [9] in minimising the corrosion of mild steel in 1M HCl

Methods

Material selection

Mild steel (MS) specimens of the following chemical composition in wt % - carbon 0.13%, manganese 0.23%, silicon 0.03%, phosphorus 0.03%, sulphur 0.016%, chromium 0.022%, nickel 0.012% and iron 99.95% were used for the entire study. Mass loss and electrochemical studies were carried out for assessing the efficacy of the inhibitor. For mass loss study, MS specimens of size 1 x 5 cm^2 were used. MS specimens with an exposed area of 1 cm^2 were used for electrochemical study. The specimens were mechanically polished, degreased, dried and stored in a desiccator.

Preparation of plant extracts
Spathodea campanulata leaves (SCL) and flowers (SCF) were collected from Thadagam area in Coimbatore and shade dried. The plant specimen was authenticated in Botanical Survey of India (BSI/SRC/5/23/2012-2013/Tech/1708) and a voucher specimen has been deposited in our university for further reference. 25 g of the dried leaves / flowers were refluxed with 500 mL of 1 M HCl for 3 hours and kept overnight. The cooled extracts were filtered and made up to 500 mL (5% extract).

Characterisation of the extract
Phytochemical examinations were carried out for the extracts as per the standard procedures mentioned [10].

Mass loss method
Pre weighed test pieces were immersed in triplicate in 100 mL of the solution containing various concentration of the inhibitor and in the absence of inhibitor for a predetermined time period as per **ASTM G 1-2**[11]. The test specimens were removed and then washed with de-ionised water, dried and reweighed.

Electrochemical measurements
Potentiodynamic measurement-Tafel polarization curves were recorded using computerized
Solartron model 1280 B. In this setup a three electrode system comprising of a platinum electrode, calomel electrode and MS specimens as auxiliary, reference and working electrodes respectively were immersed in acidic medium in the presence and absence of different concentration of the inhibitor **(ASTM G 1-2)**.

Impedance Spectroscopy:
The impedance spectral response of mild steel in the absence and presence of SCL and SCF extracts were recorded by means of Solartron electrochemical analyser 1280B. Electrochemical impedance measurements were carried out in a three electrode system with a platinum electrode as the counter electrode and a saturated calomel electrode as the reference electrode and MS sample as the working electrode. The experiments were carried out over a frequency range of 20 kHz to 0.1Hz at open circuit potential.

SEM:
Scanning electron microscopy (SEM) JEOL MODEL JSM 6360 was used to examine the morphology of the metal surface in presence and absence of the inhibitors.

FTIR Spectral Analysis
FTIR was recorded using Nexus 670/ Thermo Electron Corporation Spectrometer which extended from 4000 and 400 cm^{-1}. The interaction between the organic molecules and the metal surface has been studied by FTIR spectra.

Laser Profilometer
Surface profiles and pores were studied using a Zeta-20 3D Optical Profiler was used. MS specimens kept in a vacuum desiccator after the inhibition test were mounted on sample holder occurred under the objective of the Optical Profiler and the 3D photos were taken from the 100x magnified surface via operating program on computer. The MS specimens after exposure to 1 M HCl solution in the absence and presence of SCL / SCF extracts for 3h were examined by Zeta 3D Profiler.

Results and Discussion:

Electrochemical measurements

Potentiodynamic polarisation studies of Mild steel (MS) in the presence of SCL&SCF in 1M HCl
The potentiodynamic polarisation curves reflect a slight change in the anodic (b_a) and cathodic (b_c) curves in the presence of various concentrations of SCL (Figure 1 and Table 1). This supports the view that the inhibitor is able to suppress both the anodic dissolution and cathodic hydrogen evolution. The results indicate a considerable reduction in the I_{corr} values in the presence of the inhibitor. Inspection of the data shows that I_{corr} values decrease from 0.0075A/cm^2 to 0.0006 A/cm^2. This confirms the inhibitive nature of the extract and also the adsorption of the plant extract on the metal surface. [12]**.** A maximum of 92.0 percentage of inhibition is obtained with 0.7% concentration. Addition of extract can be seen to shift E_{corr} toward more positive values, as well as reduce the current densities of the cathodic as well as anodic reactions, which correspond to a mixed-type mechanism.[13]

The R_p values are found to vary from 4.2 Ohm/cm^2 for that of the uninhibited solution to 28.4 Ohm/cm^2 for the optimum concentration of the inhibitor (0.7% SCL) affording an efficiency of 85.2 percentage. This is indicative

of the adsorption of the active constituents of SCL onto the metal surface which creates a physical barrier for mass and charge transfer thereby providing a high degree of protection for the metal surface.[14]

Table 1 Potentiodynamic polarisation parameters for the corrosion of MS in the absence and presence of SCL/SCF in 1M HCl

S.No.	Conc. (%)	Tafelpolarisation parameters					Linear polarisation resistance parameters	
		E_{corr} mV/ SCE	I_{corr} A/cm^2	b_a mV/ decade	b_c mV/ decade	IE (%)	R_p Ohm/cm^2	IE (%)
				SCL				
1.	Blank	-496	0.0075	89	141	-	4.2	-
2.	0.1	-483	0.0040	97	112	46.7	4.8	12.5
3.	0.2	-487	0.0028	92	129	62.7	9.9	57.6
4.	0.3	-479	0.0010	99	129	86.7	22.4	75.9
5.	0.4	-480	0.001	89	131	86.7	22.6	81.3
6.	0.5	-485	0.0009	95	128	88.0	24.0	82.5
7.	0.6	-485	0.0007	85	130	90.7	28.0	85.0
8.	0.7	-498	0.0006	88	135	92.0	28.4	85.2
				SCF				
1.	Blank	-496	0.0075	89	141	-	4.2	-
2.	0.1	-478	0.0040	87	117	46.7	8.5	50.6
3.	0.2	-487	0.0032	81	123	57.3	8.7	51.7
4.	0.3	-475	0.0025	96	143	66.7	10.0	58.0
5.	0.4	-476	0.0027	93	143	64.0	11.4	63.2
6.	0.5	-478	0.0024	94	149	68.0	12.9	67.4
7.	0.6	-475	0.0020	92	143	73.3	13.5	68.9
8.	0.7	-474	0.0016	82	154	78.7	14.4	70.8

In the case of SCF, an increase in inhibitor concentration led to a decrease inI_{corr} values from 0075 A/cm^2 (blank) to 0.0016 A/cm^2 (0.7% SCF). A maximum of 78.7 percentage of inhibition is obtained with 0.7% concentration. This behaviour indicates the protective nature of the extract.

No significant change in E_{corr} values are observed in the presence of SCF. Generally an inhibitor can be classified as a cathodic /anodic inhibitor if the shift is more than 85 mV with respect to that of blank. In the present case, the E_{corr} values are less than 85 mV from the blank value, demonstrating the mixed nature of the inhibitor.[15] Linear Polarisation resistance values (R_p) show an increase in value from 4.2 ohm/cm^2 for that of blank to 14.4 ohm/cm^2 for 0.7 % of SCF. Increase in R_p with concentration infers that the active constituents of SCF inhibit corrosion of MS by adsorption process. Maximum increase in R_p values is noticed at 0.7% SCF with an efficiency of 70.8percentage.

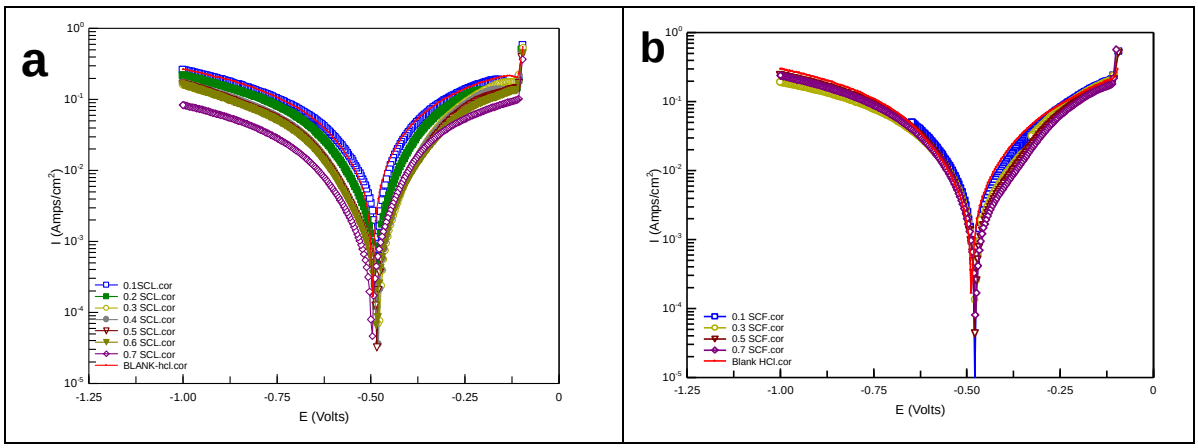

Figure 1 Potentiodynamic polarisation curvesfor MSin 1 M HCl in absence and presence of (a) SCL (b) SCF extracts

Electrochemical Impedance Measurements

The EIS technique has been one of the methods used to report the mechanism of corrosion and corrosion protection of metals and alloys in aggressive media. Impedance measurements provide an insight into the kinetics of interfacial mass transfer process [16].

The impedance profile in uninhibited acid (Figure -2) reflects a single capacitive semicircle. Analyses of the spectra also reveal that they are not perfect semicircle in nature. This anomalous behaviour may be attributed to surface roughness, distribution of the active sites or due to the adsorption of the inhibitor species**.** The diameter of the semi circle increases with increase in concentration of the studied inhibitor and the shape of the semi circle does not change in the presence of the inhibitor implying that there is no change in the mechanism of MS dissolution in the presence of SCL /SCF. The results reflect that the R_{ct} values increase(from 30.4 Ωcm^2 to 224.4 Ωcm^2) with increase in concentration of inhibitor (Table 2)to afford a maximum efficiency of 86.5 percentage for SCL and in the case of SCF .This might be due to the adsorption of the phytochemical constituents adsorbed onto the MS surface. The corresponding Bode plots show only one maximum phase reflecting one time constant. This is indicative of one step mechanism [17] The value of C_{dl} decreases with inhibitor concentration.This decrease in value C_{dl}which results from a decrease of dielectric constant and/or increase in thickness of double layer suggests that the inhibitor molecules function by adsorptionat acid/metal interface [18]

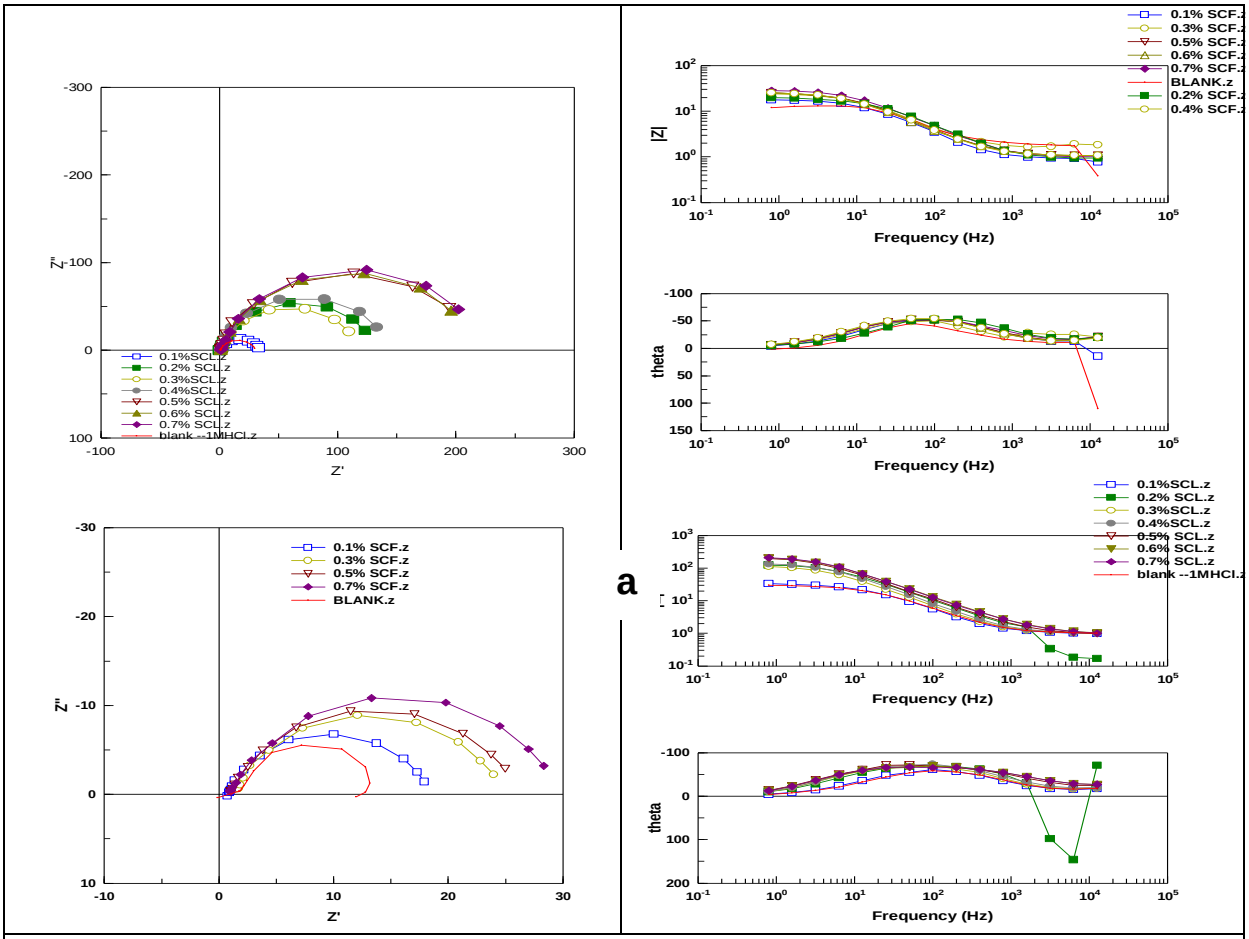

Figure 2 Nyquist and Bode diagrams for MS Electrode in 1M HClin the absence and presence of (a)SCL (b) SCF

The impedance function of a CPE is defined by the mathematical expression given below:

$$Z_{CPE} = Y_o^{-1} (i\omega)^{-n} \quad (1)$$

where Y_o is the CPE constant (in $\Omega^{-1} s^n cm^{-2}$), ω is the sine wave modulation angular frequency (in rad s^{-1}), $i^2 = -1$ is the imaginary number, $n=\alpha/(\pi/2)$ in which α is the phase angle of CPE and n is the CPE exponent ($0 \leq n \leq 1$) which measures the deviation from the ideal capacitive behaviour and it represents the surface irregularity. [19,20]

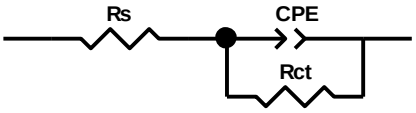

Figure 3 Proposed equivalent circuit model

The values of double layer capacitance $C_{dl}$for a circuit including CPE are calculated according to the following equation

$$C_{dl} = (Y_o\omega_{max})^{n-1} \textbf{(2)}$$

Where $\omega_{max}$is angular frequency ($\omega_{max}= 2\pi f_{max}$) at which the imaginary part of the impedance is maximal and $f_{max}$is AC frequency at maximum. [21]

The impedance parameters, namely charge-transfer resistance (R_{ct}), solution resistance (R_s), the constant phase element (Y_o) related to the capacity of the double layer and the exponent (n), relevant to the capacitive semicircle of from the mild steel/ 1M HCl/SCL/SCF extracts are listed in Table 2. These parameters are calculated the non-linear least square fit of the equivalent circuit as depicted in Figure-3. Simulation of Nyquist plots with above model shows an excellent agreement with experimental data.

The relaxation time (τ) of the surface, that is, the time required for attaining the charge distribution to equilibrium is given by:

$\tau = C_{dl} \times R_{ct}$

The adsorption of inhibitor needs some time to attain equilibrium. This time is very short, as shown in Table 2. In 1MHCl containing different inhibitor concentration, τ increases with increase of inhibitor concentration which means slow adsorption process [22]

Table 2 Electrochemical Impedance parameters for corrosion of MS in the absence and presence of SCL and SCF in 1M HCl at room temperature

(%)	R_S (Ωcm^2)	Y_0 ($\mu F/cm^2$)	n	R_{ct} (Ωcm^2)	IE (%)	f_{max} (μHz)	CPE/C_{dl} ($\mu F/cm^2$)	θ	τ (S^n)
SCL									
Blank	0.861	5399	0.93	30.4	-	15.4	365		0.011
0.1	0.826	4901	0.96	33.9	10.6	12.87	341	0.07	0.012
0.2	0.053	2458	0.97	64.9	53.2	7.6	323	0.12	0.037
0.3	0.959	3115	1.13	118.4	74.4	4.287	314	0.14	0.037
0.4	0.939	2817	1.14	142.7	78.7	4.353	256	0.3	0.046
0.5	0.748	1233	1.17	217.6	86.0	3.428	213	0.41	0.042
0.6	1.289	1123	1.16	218.5	86.1	3.796	192	0.47	0.043
0.7	1.402	767	1.16	224.4	86.5	3.73	190	0.48	0.04
SCF									
Conc (%)	R_S (Ωcm^2)	Y_0 ($\mu F/cm^2$)	n	R_{ct} (Ωcm^2)	IE (%)	f_{max} (μHz)	CPE/C_{dl} ($\mu F/cm^2$)	θ	τ (S^n)
Blank	-0.63	40110	0.50	4.0	-	55.6	721.7		0.003
0.1	0.95	10566	0.82	15.1	73.5	20.4	517.8	0.28	0.008
0.2	1.00	9633	0.84	16.5	75.8	19.0	507	0.30	0.008
0.3	1.77	8272	0.87	19.3	79.3	16.5	500	0.31	0.010
0.4	1.15	7469	0.89	21.3	81.2	15.2	492	0.32	0.010
0.5	1.15	7674	0.88	20.8	80.8	16.5	465	0.36	0.010
0.6	1.16	7648	0.89	20.8	80.8	15.3	499	0.31	0.010
0.7	1.11	6756	0.89	23.6	83.1	19.3	350	0.52	0.008

Mass Loss Method

The effect of SCL extract on the corrosion inhibition of MS is tested by mass loss measurements. Table 3 shows the variation of corrosion rate and inhibition efficiency with increase in concentration of the inhibitor. It can be

seen from the table that the corrosion rate decreases with increasing concentration of the inhibitor. The IE of the inhibitor increases from 54.9 percentage at 0.1% SCL to 88.4 percentage at 0.7 % of SCL.

Table 3 Inhibition efficiency as a function of immersion time and concentration of SCL /SCF in 1M HCl

Conc. %	1/2 h		1h		3h		6h		12h		24h	
	CR (mpy)	IE (%)	CR (mpy)	IE (%)	CR (mpy)	IE (%)	CR (mpy)	IE (%)	CR (mpy)	IE (%)	CR (mpy)	IE (%)
SCL												
Blank	1032		1190		1238		2197		1561		1209	
0.1	465	54.9	290	75.6	246	80.1	147	93.3	422	73.0	595	50.8
0.2	432	58.1	188	84.2	182	85.3	120	94.5	202	87.1	311	74.3
0.3	380	63.2	166	86	133	89.2	117	94.7	137	91.2	278	77.0
0.4	300	70.9	154	87.1	107	91.4	70	96.8	134	91.4	232	80.8
0.5	245	76.3	149	87.5	84	93.2	57	97.4	124	92.0	149	87.7
0.6	182	82.4	128	89.2	60	95.2	48	97.8	69	95.6	135	88.8
0.7	120	88.4	107	91	40	96.8	43	98.0	24	98.5	76	93.7
SCF												
Blank	1032		1190		1238		2197		1561		1209	
0.1	321	68.9	563	52.7	223	82.0	439	80.0	337	78.4	515	57.4
0.2	295	71.4	495	58.4	202	83.7	198	91.0	229	85.3	491	59.4
0.3	269	73.9	450	62.2	181	85.4	165	92.5	200	87.2	480	60.3
0.4	251	75.7	279	76.6	137	88.9	110	95.0	156	90.0	466	61.4
0.5	213	79.4	182	84.7	126	89.8	105	95.2	147	90.6	310	74.4
0.6	168	83.7	145	87.8	87	93.0	97	95.6	117	92.5	238	80.3
0.7	136	86.8	139	88.3	67	94.6	92	95.8	97	93.8	193	84.0

An insight into the stability of SCL extract with time may be gained by studying the effect of the extract on MS specimen for various time of immersion. The results evaluated for the variation of mass loss with exposure time for the MS specimen immersed in 1M HCl with and without inhibitors are presented in Table 6. From the table, it can be seen that a maximum IE of 98.5 percentage is maintained till 12 h and thereafter a slight decline is observed and the efficiency stabilises to 93.7 percentage at 24h for the extract. Similarly in the case of SCF, it can be seen that a maximum IE of 95.8 percentage is maintained till 6 h and thereafter a slight decline is observed. But the inhibition efficiency is found to stabilise at 24h to afford an efficiency of 84 percentage demonstrating the effectiveness of the inhibitor at longer periods of immersion. The IE of the studied extracts increase with increasing time of immersion upto 6h (12h for SCL) and then decrease to finally stabilise at 24h to afford 84- 93 percentage.

This behaviour can be discussed on the basis that prolonged immersion of MS in acid solution a) allows the cathodic or hydrogen evolution kinetics to increase presumably or more cathodic or carbon containing sites are exposed by the corrosion process b) increase the concentration of ferrous ions which decrease the corrosive nature of the acid. [23]

Effect of temperature:

Interaction between the metal electrode and the corrodent acidic medium is alters significantly in the presence of inhibitors. To assess the impact of temperature on corrosion and corrosion inhibition process, mass loss measurements are carried out in the range of 303 to 353K.The collected results are tabulated and discussed.

Table 4 presents the variation of the inhibitor efficiency of SCL and SCF with temperature in 1M HCl. It can be seen that, the presence of SCL and SCF in 1M HCl, decreases the corrosion rate of MS at any given temperature with increase in inhibitor concentration. In contrast at constant inhibitor concentration, the corrosion rate increases with a rise in temperature. Analysing the temperature effect of SCL and SCF, the IE increases with increase in temperature up to 323K giving rise to 94.1percentage for SCL and 93.1 percentage for SCF and then a slight decrease is noted at 333 to 343K which then stabilises to 87.4 percentage for SCL and 82.2 percentage for SCF at 353K. This might be due to desorption of the adsorbed inhibitor molecules at elevated temperatures[24].

Table 4 Effect of concentration of SCL/SCF on Inhibition efficiency at various temperatures

Conc %	Temperature (K)											
	303		**313**		**323**		**333**		**343**		**353**	
	CR (mpy)	**IE (%)**	**CR (mpy)**	**IE (%)**	**CR (mpy)**	**IE (%)**	**CR (mpy)**	**IE (%)**	**CR (mpy)**	**IE (%)**	**CR (mpy)**	**IE (%)**
SCL												
Blank	1032		2755		6252		8146		9971		18091	
0.1	465	54.9	995	63.9	2244	64.1	3284	59.7	4785	52.0	8180	54.8
0.2	432	58.1	798	71	1638	73.8	2491	69.4	4606	53.8	6491	64.1
0.3	380	63.2	696	74.7	1413	77.4	2158	73.5	3813	61.8	6141	66.1
0.4	300	70.9	517	81.2	988	84.2	1757	78.4	2849	71.4	5297	70.7
0.5	245	76.3	457	83.4	819	86.9	1390	82.9	2311	76.8	4359	75.9
0.6	182	82.4	355	87.1	600	90.4	1041	87.2	1655	83.4	3403	81.2
0.7	120	88.4	201	92.7	369	**94.1**	887	89.1	1100	89.0	2279	87.4
SCF												
Blank	1032		2755		6252		8146		9971		18091	
0.1	321	68.9	601	78.2	913	85.4	1605	80.3	4188	58.0	6676	63.1
0.2	295	71.4	568	79.4	625	90.0	1287	84.2	3829	61.6	4432	75.5
0.3	269	73.9	518	81.2	606	90.3	1246	84.7	3470	65.2	4233	76.6
0.4	251	75.7	449	83.7	556	91.1	1214	85.1	3121	68.7	4179	76.9
0.5	213	79.4	394	85.7	544	91.3	1165	85.7	2353	76.4	3672	79.7
0.6	168	83.7	320	88.4	469	92.5	1035	87.3	1924	80.7	3600	80.1
0.7	136	86.8	270	90.2	431	**93.1**	937	88.5	1585	84.1	3220	82.2

Langmuir Adsorption model for investigated inhibitors:

Langmuir adsorption equation relates degree of surface coverage to concentration of inhibitor according to equation (3).

$$\text{Log } (C/\theta) = \log C - \log K \qquad \textbf{(3)}$$

A plot of log (θ/1-θ) versus log C from mass loss data obtained for studied inhibitors yields straight lines as represented in Figure 4. The slope deviates from unity. This deviation may be explained on the basis of the interaction among adsorbed species on the metal surface. It has been postulated in the derivation of Langmuir adsorption isotherm equation that adsorbed molecules do not interact with one another, but this is not the case of large organic molecules having polar atoms (or) groups which can adsorbed on the cathodic and anodic sites of the metal surface such adsorbed species interact by mutual repulsion or attraction [25]**.** It is also possible that the inhibitor studied can be adsorbed on the anodic and cathodic sites resulting in deviation from unit gradient.

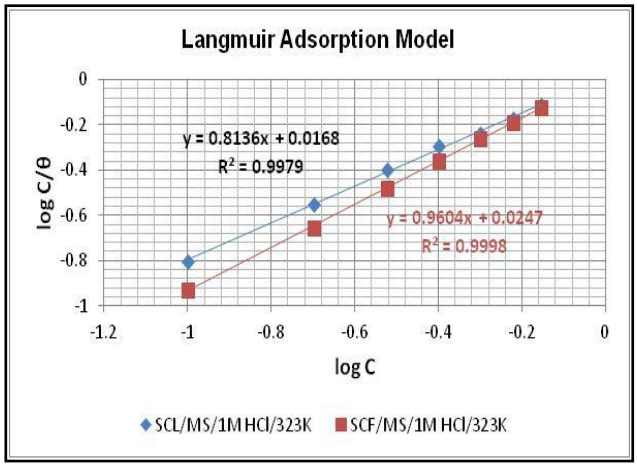

Figure 4 Langmuir Adsorption Isotherm

Energy of Activation

The dependence of corrosion rate on temperature can be regarded as an Arrhenius – type process, the rate of which is given by

$$\log CR = \log A - E_a/2.303RT \quad (4)$$

where CR is the corrosion rate of MS, A is Arrhenius or pre-exponential constant, $E_a$is the activation energy for the corrosion of MS, R is the gas constant and T is the temperature.

Figure 5a depicts Arrhenius plot as log of corrosion rate (log CR) against the reciprocal of temperature (1/T) for MS in 1M HCl in the free acid solution and the acid containing different concentrations of SCL / SCF extracts.

The apparent activation energy for the corrosion of **MS** in 1M HCl is calculated from the Arrhenius plot of log CR against 1/T in the absence and presence of different concentrations of SCL/SCF. The E_a values are deduced from the slopes of these lines and the values of $E_a$for various concentrations of the inhibitors are tabulated in Table 5

It can be seen in the table that E_a is higher in the presence of the inhibitors than in their absence. The modification in the values of E_a may be attributed to the geometric blocking effect of adsorbed inhibitive species on the metal surface [26]. This observation further supports the proposed physisorption mechanism as reports [27] show that lower values of E_a in the presence of inhibitors in comparison to the free acid solution are indicative of chemical adsorption mechanism, whereas the opposite suggests a physical adsorption mechanism.

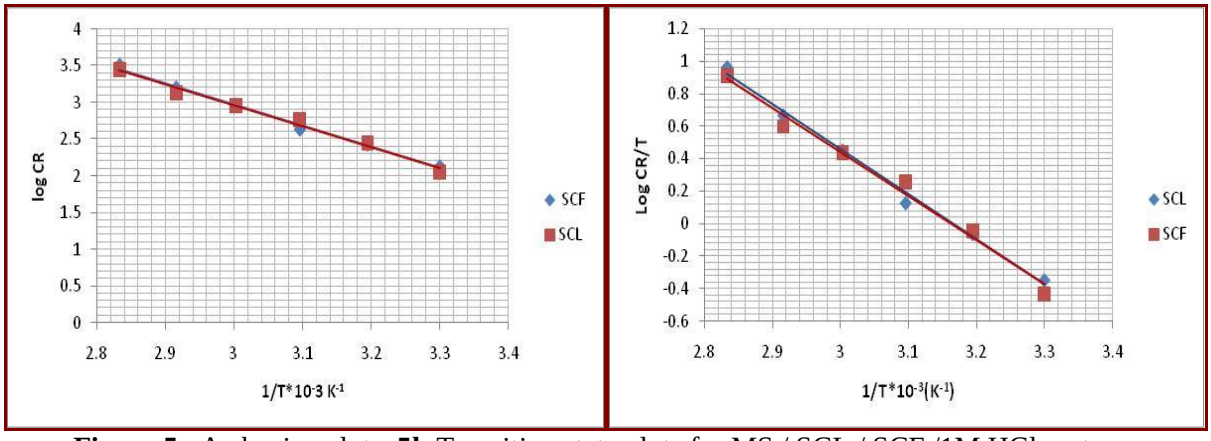

Figure 5a Arrhenius plots; **5b** Transition state plots for MS / SCL / SCF /1M HCl systems

Further evidence regarding the kinetic and mechanistic process of the corrosion mechanism can be realised from the values of apparent activation energy[28]. Inspection of Table also reveals that E_a increases with increase in SCL / SCF extracts. Activation energy values for the investigated inhibitors are found to be higher than the blank values, implying the increase of energy barrier for the corrosion process in the presence of the additives. This emphasizes the electrostatic nature of the adsorbed inhibitors on the **MS** surface [29].

Table 5 Activation parameters for MS corrosion in 1 M HCl in the absence and presence of different concentrations of SCL / SCF

	E_a(kJ/mol)								
Conc (%)	Blank	0.1	0.2	0.3	0.4	0.5	0.6	0.7	Average
SCL	47	50	49	49	51	50	50	53	50
SCF	47	55	51	51	52	52	54	56	53

4.5.2 Entropy of Activation and Enthalpy of Activation

In order to calculate the enthalpy, ΔH_a and entropy, ΔS_a of activation for the corrosion process, the alternative formulation of Arrhenius equation, also called transition state equation, is used:

$$\frac{CR}{T} = \frac{R}{Nh}\exp\left(\frac{\Delta Sa}{R}\right)\exp\left(\frac{\Delta H}{RT}\right) \quad (5)$$

where h is the Planck's constant, N is the Avogadro's number, ΔS_a is the entropy of activation, T is the absolute temperature and R is the universal gas constant. The relationship between log (CR/T) versus 1/T for **MS** corrosion in 1M HCl in the absence and presence of different concentrations of SCL/SCF extract is shown in Figure 5b.

Straight lines are obtained with slope of ($-\Delta H_a/2.303R$) and an intercept of ($\log R/Nh + \Delta S_a/2.303R$) from which the values of ΔH_a and ΔS_a respectively are computed and listed in Table 6.

Table 6 Average values of activation parameters for MS corrosion in 1 M HCl in the absence and presence of SCL/SCF

Inhibitor	E_a (kJ/mol)	ΔH_a (kJ/mol)	ΔS_a (J/mol K^{-1})
Blank	47	44.6	-37.9
SCL	50	47.2	-40.8
SCF	53	49.5	-35.5

The Table reflects that $E_a$and ΔH_a are close to each other as expected from transition state theory concept and they are also found to vary in a similar manner in the presence of the inhibitors. It is also seen in Table 6 that E_a and ΔH_a vary in the same manner but however, the values of ΔH_a are lower than that of E_a. This has been reported [30] to indicate that the corrosion process must involve a gaseous reaction, simply hydrogen evolution reaction associated with decrease in total reaction volume.The positive values of ΔH_a both in the absence and presence of additives reflect the endothermic nature of the steel dissolution process and it indicates that the dissolution of **MS** is difficult [31].

The values of ΔS_a in the absence and presence of the extracts are negative for **MS** (Table 6). This implies the inhibitor molecules, freely moving in the bulk solution are adsorbed in an orderly fashion onto the **MS** surface. This infers that the activation complex in the rate determining step represents as association rather than a dissolution step, meaning that a decrease in disordering takes place on going from reactants to the activated complex [32]**.**

Thermodynamic Adsorption Parameters

Thermodynamic model is very useful to explain the adsorption phenomenon of inhibitor molecule. A plot of ΔG^o_{ads} versus T is linear (**Figure 6**) for MS acid corrosion in the presence of various concentrations of investigated extracts in 1M HCl. The slopes of the straight lines are equal to ΔS^o_{ads} and intercept equal to ΔH^o_{ads}. Figure 6 clearly shows the dependence of ΔG^o_{ads} on T, indicating good correlation among thermodynamic parameters

Table 7 Thermodynamic adsorption parameters for MS corrosion in 1 M HCl in the absence and presence of SCL/SCF

Inhibitor	Free energy of adsorption ΔG^o_{ads} (kJ/mol)						ΔS^o_{ads} J/mol	ΔH^o_{ads} kJ/mol
	303K	313K	323K	333K	343K	353K		
SCL	-15.9	-18.0	-19.2	-17.9	-18.4	-18.2	-26.7	-9.2
SCF	-15.7	-17.1	-18.7	-17.7	-17.2	-16.8	-13.0	-12.95

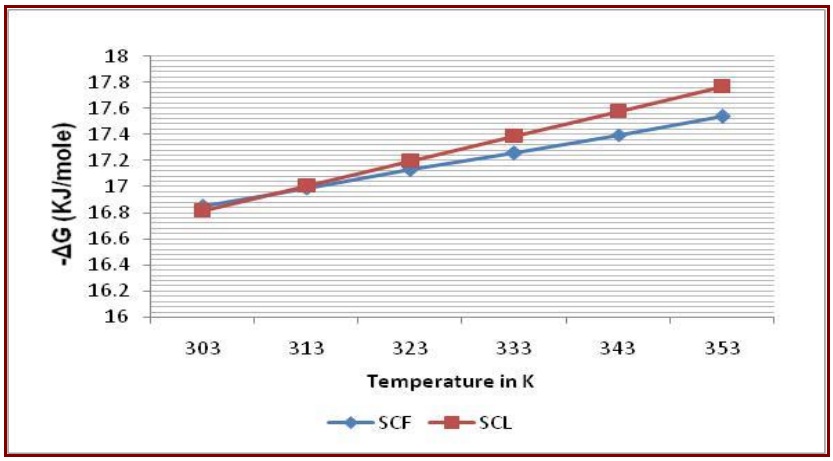

Figure 6 Best fit curves of $-\Delta G°_{ads}$Vs T for MS / SCL/ SCF 1MHCl

4.6.1 ΔG^{o}_{ads}

The calculated mean values of ΔG^{o}_{ads},ΔH^{o}_{ads}, ΔS^{o}_{ads}at all the investigated temperatures (303-353K)for different concentration of SCL / SCF extracts are represented in Table 7. **Figure 7** clearly shows the dependence of ΔG^{o}_{ads} on T, indicating the good correlation among thermodynamic parameters. The large and negative values ofΔG^{o}_{ads} ensure the spontaneity of the adsorption process and stability of the adsorbed layer on the steel surface [33].

The calculated value of ΔG^{o}_{ads} presented in Table 7, are negative which indicate that the adsorption of inhibitormolecules on the metal surface is a spontaneous process. Generally, values of ΔG^{o}_{ads} around -20 kJmol^{-1} or lower are consistent with the electrostatic interaction between the charged molecules and the charged metal p(hysisorption); those around -40 kJmol^{-1} or higher involve charge sharing or transfer from organic molecules to the metal surface to form a coordinate type of bond (chemisorption) [34]. In the present work, the calculated ΔG^{o}_{ads} values are almost slightly less negative than -20 kJmol^{-1} ranging from -15 to -19 kJmol^{-1}. Hence it may be assumed that the adsorption of the inhibitor molecules is obeying physical adsorption however chemical adsorption may not be excluded due to the complex nature of the corrosion inhibiting process [35].

ΔH^{o}_{ads} and ΔS^{o}_{ads}

The negative sign of ΔH^{o}_{ads} indicated that the adsorption of the inhibitors on metal surface was exothermic in nature [36]. The entropy of adsorption $\Delta S^{o}_{ads}$for the system SCL / SCF in 1M HCl are negative because the inhibitor molecules freely moving in the bulk solution, are adsorbed in an orderly fashion onto the mild steel surface, resulting in a decrease in entropy **.**Inspection of Table 7 reveals that decrease in enthalpy and entropy is the driving force for the adsorption of SCL / SCF in 1M HCl on the MS surface [37]

FT-IR Spectral studies

The FT- IR spectrum of the corrosion product after 3h of immersion in 1M HCl in the presence of the inhibitor is depicted in Figure 7a. The band observed at 3394cm^{-1} (for that of the SCL extract) is shifted to 3603 cm^{-1}and the –CH_2 asymmetric band at 2924cm^{-1} is shifted to 3117 cm^{-1}. A band at 2376 cm^{-1} attributed to C ≡ N stretching observed in the plant spectra shifts to 2315 cm^{-1} in the corrosion product. The absorption band at 1628cm^{-1} (C=O stretching) diminishes and shifts to 1636 cm^{-1}.A peak noticed for C-Ostretching at 1072cm^{-1}shifts to 1057 cm^{-1} The shift in the absorption frequencies of the inhibitor on the metal surface strongly supports the interaction between the phytochemical compounds of the inhibitor and metal surface. Bands at 450 cm^{-1} to 700 cm^{-1} probably originates mainly from γ -Fe_2O_3 (702 cm^{-1}). Some bonds are missing in the spectrum of the corrosion product indicating that these bonds might have been involved in bonding .

Analysis of the IR spectral data of SCF reflects that a band noticed at 3950 cm-1 shifts to 3981 cm^{-1} in the corrosion product. Bands at 2376 cm^{-1} and 1628 cm^{-1} pertaining to C≡N stretching and C=O stretching are noticed in the corrosion product also. Also a shift from 1427 cm^{-1} to 1520 cm^{-1} is noted for C-H bending .Some bonds, for example 1381 cm^{-1} corresponding to C-O-C stretching disappears in the corrosion product. A band for C-O stretching assigned to 1265 cm^{-1} is downshifted to 1211 cm^{-1} in the corrosion product and a band at 1065 cm^{-1} identified as a C-O stretching vibration disappears in the corrosion product. A band pertaining to OH bending noted at 772 cm^{-1} is shifted to 826 cm^{-1} in the corrosion product.

These progressive shifts in the wavelength indicates that there is interaction (Fe-SCL /SCF complex formation) between SCL / SCF and the surface of MS [38,39] .

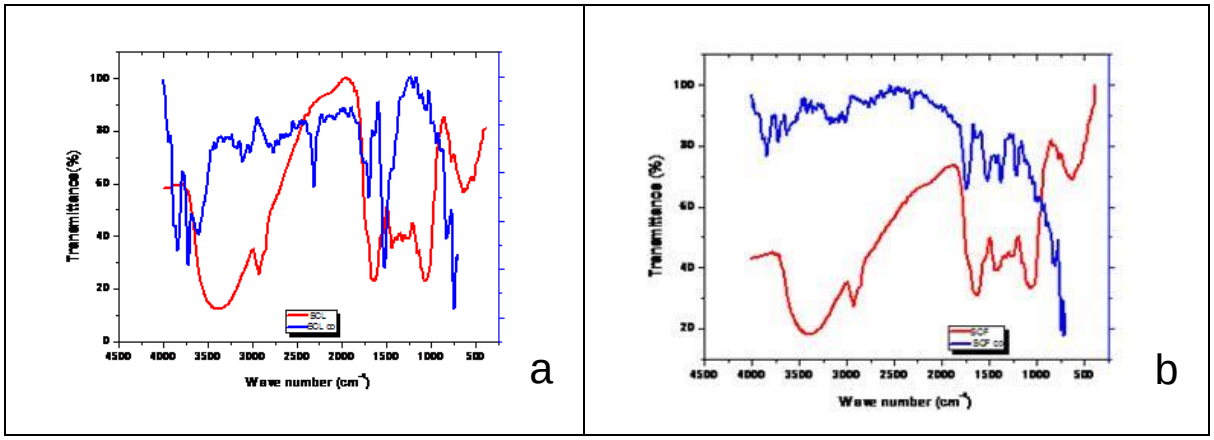

Figure 7 FT-IR Spectrum of (a) SCL and corrosion products in the presence of SCL (b) SCF and corrosion products in the presence of SCF

Scanning Electron Microscopic studies (SEM)

Scanning electron microscope images of the surface of the **SCL/SCF /MS/1M HCl** samples are taken to study the morphology before and after the inhibition process. Cleaned MS sample surfaces show few defects and sub micrometer cracks over the surface as shown in Figure 8 a. Deep corrosion and considerable loss of the surface material is noticed when the MS sample is treated in 1M HCl as shown in Figure 8 b. [40]. However, a significant decrease in the loss of surface material is observed in presence of inhibitor (0.7% SCL and SCF) for same time period. It can be noted that the corrosion is tangibly suppressed resulting in a smoother surface similar to that of the original specimen (Figure 8 c,d) This enhancement of surface morphology indicates the formation of a good protective film of SCl/SCF on MS surface that is responsible for inhibition [41]**.**

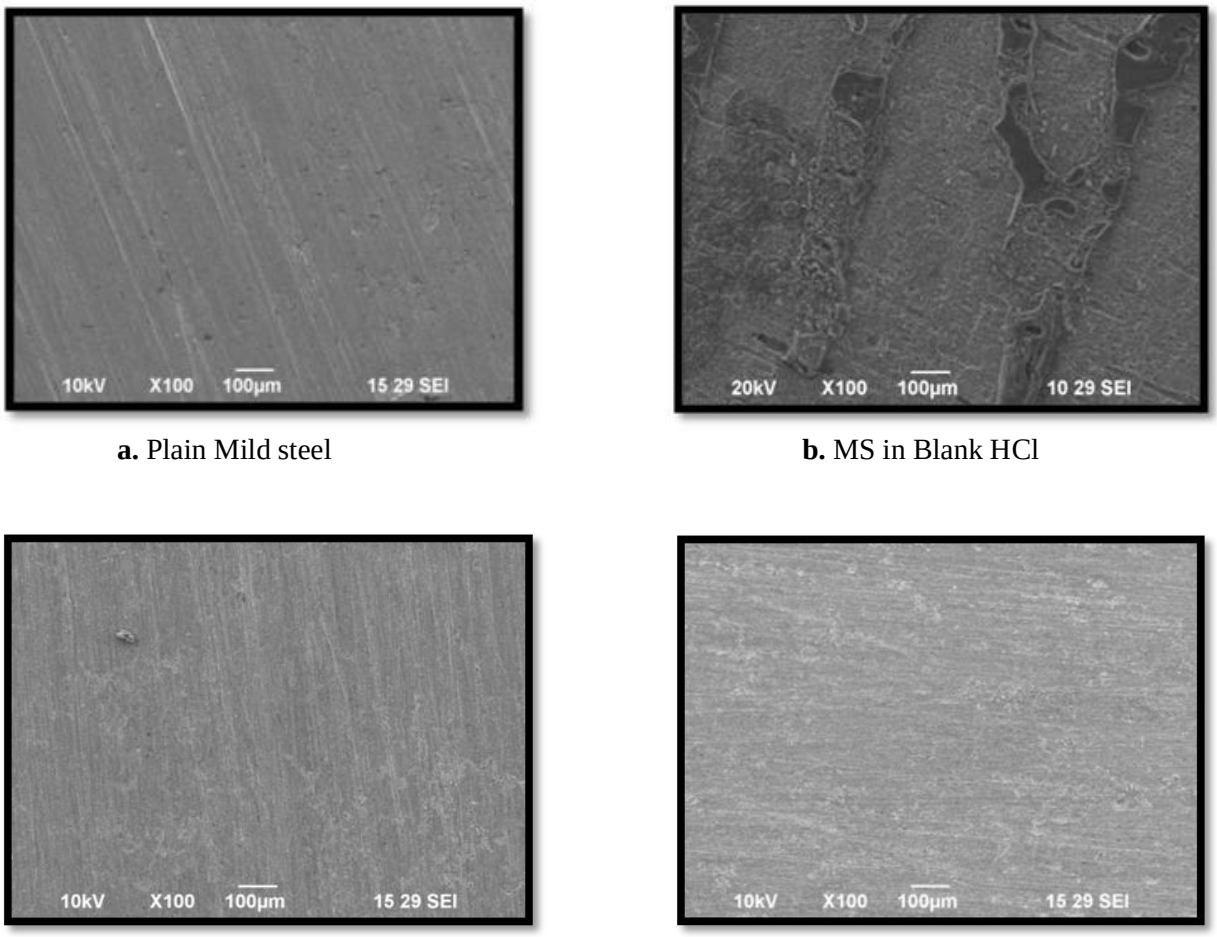

a. Plain Mild steel **b.** MS in Blank HCl

c. MS /SCL/ 1M HCl **d.** MS /SCF / 1M HCl

Figure 8 SEM pictures of SCL/SCF/MS/1M HCl

Energy dispersive X-ray analysis (EDX)

Figure 9 represents the EDX profile analysis and percentage of atomic content in MS samples, respectively. The characteristicpeaks of the elements constituting the MS in absence and presence of 0.7% optimum concentration of SCL/SCF extracts are displayed in tables along with the EDX Figures (Figures 9 a -d)

The analysis infers that the characteristic peaks of elements constituting polished MS samples comprises of major Fe peaks with Mn, Si & P as minor constituents. The presence of Si may be attributed to the mechanical abrasion of the MS surface prior to the experiment.

For MS in the presence of 1M HCl the EDX analysis reported 9.89% Fe & 90.11% Oxygen (in weight %). The detection of small peak characterizing oxygen is detected due to the formation of iron oxide layer due to the immersion of MS in 1M HCl medium. The low content of Fe when compared to the iron content in plain MS surface and the absence of Mn and the presence of high oxygen concentration indicates that the MS surface is completely covered with a thick layer of corrosion product [42]**.**

The EDX patterns in the presence of SCL/SCF give an additional peak due to presence of S. The presence of S peaks in the EDX patterns of inhibitors on the surface indicates that the inhibitor is adsorbed on the MS surface, preventing it from being corroded [43].

a. PlainMS

Element	Wt %	At %
Si	0.35	0.69
P	0.10	0.18
Mn	2.38	2.41
Fe	97.17	96.72

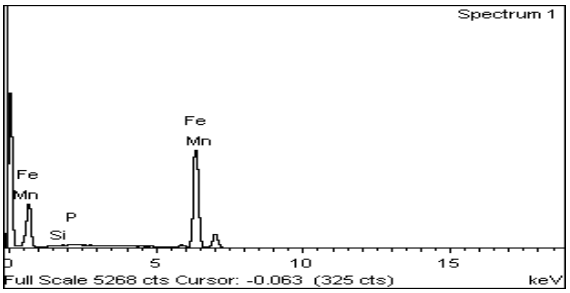

b. BlankHCl

Element	Wt %	At %
O	9.89	27.70
Fe	90.11	72.30

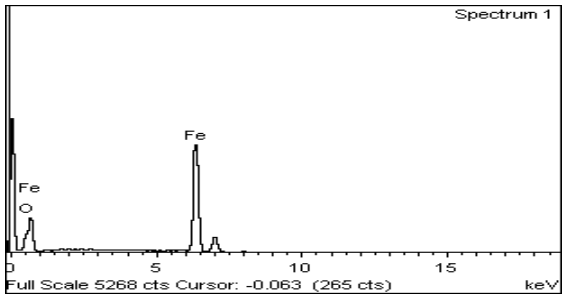

c. MS /SCL/ 1M HCl

Element	Wt %	At %
O	1.79	1.36
S	0.20	0.30
Fe	86.9	64.6

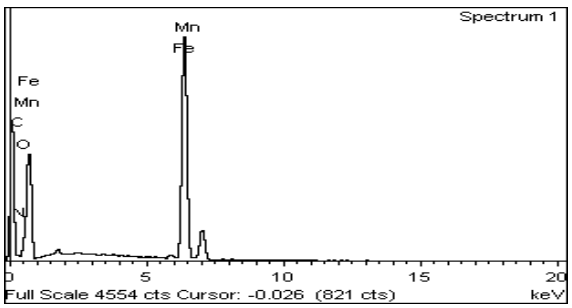

d. MS /SCF / 1M HCl

Element	Wt %	At %
O	4.47	13.27
S	0.02	0.03
Fe	91.17	77.52

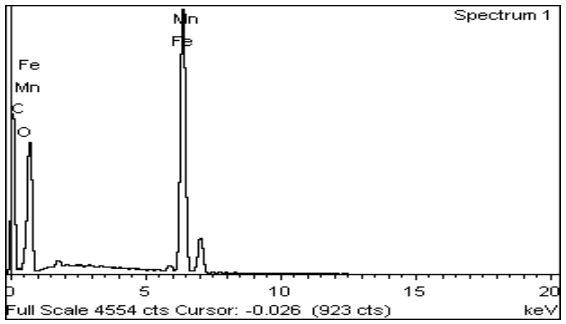

Figure 9 EDX images of MS corrosion in absence and presence of (c) SCL (d) SCF in 1M HCl

3D Optical profilometry:

It is a powerful tool to investigate the surface morphology of various samples at nano-micro scale that is currently used to study the influence of corrosion inhibitors on metal/solution interface. From the analysis, insight can be gained regarding the roughness & uniformity of the surface.

Figure 10 shows the 3D images as well as elevation profiles of polished MS and MS in 1M HCl. Figure 10 (c),(d) show that the 3D images as well as elevation profiles of MS/ 1M HCl in the presence of investigated inhibitors.

As observed in Figure 10 b the surface of MS electrode exposed to corrodent solution has a considerably porous structure with large and deep pores. Figure 10 c, d, reveals that there is wrapping zonal film adsorbed on MS surface. In accordance, it can be concluded that the adsorption film can efficiently protect the MS from corrosion [44]. The decrease in the R_a value reflects the adsorption of inhibitor molecules on MS surface thereby reducing the corrosion rate.

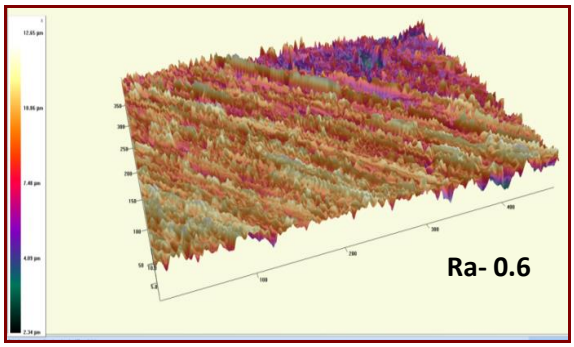

a. Plain Mild steel

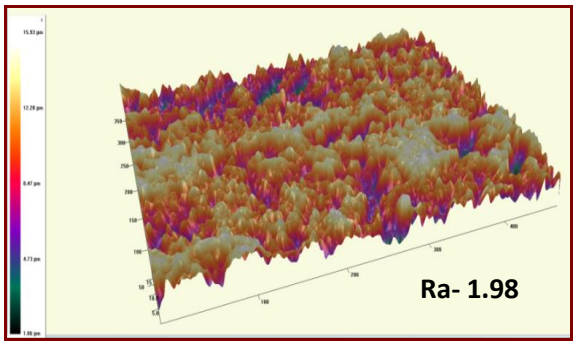

b. Blank HCl

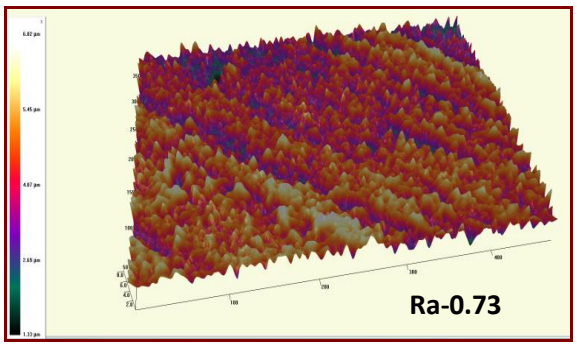

c. Mild steel /SCL/ 1M HCl

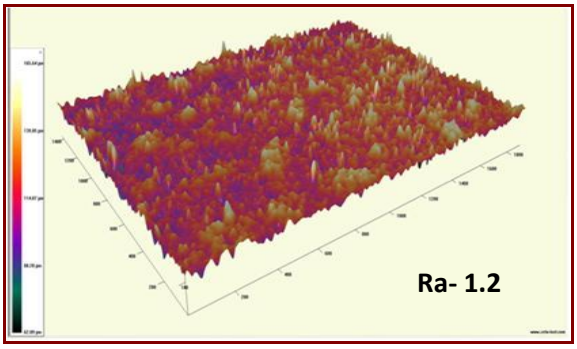

d. Mild steel /SCF/ 1M HCl

Figure 10 3D Optical Profiler images of MS in absence and presence of (c) SCL (d) SCF in 1M HCl

Proposed Mechanism for Mild Steel /1M HCl / Inhibitors

In aqueous acidic solutions, main constituents exist either as neutral molecules or as protonated molecules (cations).The inhibitors may adsorb on the metal/acid solution interface by one and/or more of the following ways:

- Electrostatic interaction of protonated molecules with already adsorbed chloride ions,
- Donor-acceptor interactions between the π-electrons of aromatic ring and vacant d orbital of surface iron atoms,
- Interaction between unshared electron pairs of hetero atoms and vacant d-orbital of iron surface atoms.

The phytochemical characteristics of SCL and SCF extracts are summarized in Table 8. The results indicate the presence of phytoconstituents like flavonoid, tannins, terpenoids, steroids and saponins in the leaves and moderate amount of flavonoids, terpenoids and anthroquinones in the flowers extract. Similar assertions are also made by [45]

Table 8 Preliminary phytochemical screening of the crude extracts

Spathodea campanulata	Phytochemical constituents							
	Flavonoids	Alkaloids	Terpenoids	Saponins	Tannins	Reducing sugar	Polyphenols	Anthroquinones
Leaves	+++	+	++	+	+	-	+	-
Flowers	+	-	+	++	-	+	+	+

+++, appreciable amount; ++, moderate amount; +, trace amount; -, not detected

The inhibition efficiency afforded by SCL /SCF may be attributed to the presence of electron rich O and N atoms. The possible reaction centers are unshared electron pair of hetero-atoms and/or p -electrons of aromatic ring. Generally, phytoconstituents can adsorb on the MS surface on the basis of donor – acceptor interactions between π (pi) electrons of the O and aromatic ring and vacant d orbitals of surface iron.[46]

Summary:

- The investigated inhibitors, performed in an effective manner to minimize the corrosion of **MS** in 1M HCl medium.
- The potentiodynamic polarisation studies reflect that the inhibitors were able to suppress both the anodic dissolution and cathodic hydrogen evolution.
- Analysis of the results of the mass loss measurements of **MS** infer that the inhibition efficiencies increased with increasing concentration of the inhibitors. The investigated inhibitors could furnish an efficiency of 90-98percentage at a maximum concentration of 0.7%.
- Surface morphology of the metal indicated the formation of protective layer of metal-inhibitor complex on the metal surface.

Acknowledgement

The authors would like to thank the authorities of Avinashilingam Deemed University for Women, Coimbatore-641043, Tamilnadu, India for providing necessary facilities for carrying out this study.

References

[1] Xianghong Li and Guannan Mu, Appl Surf Sci, 2005, 252, 1254-1265.
[2] Abiola ,O.K, James ,A.O , Corros. Sci., 2010,52 , 661.
[3] Rajalakshmi, R., Prithiba, A, Leelavathi, S , Journal of Chemica Acta, 2012a , 1(1):6-13.
[4] Subhashini S, Rajalakshmi R, Elakkiya T and Srimathi M, J Ultra Chem, 2008,4(2),159-164.
[5] Subhashini S, Rajalakshmi R, Prithiba A, Mathina. A, E-Journal of Chemistry. 2010,7(4): 1133-1137.
[6] Rajalakshmi R, Subhashini S, Prithiba A, Asian Journal of chemistry. 2010, 22 (7):5034-5040.
[7] Rajalakshmi R. Safina A. S, E-Journal of Chemistry. 2012, 9(3):1632-1644.
[8] Rajalakshmi, R ,Prithiba, A., ICGTEPC 2014
[9] Rajalakshmi, R ,Prithiba, A., NCCI 2014
[10] Harborne JB, Phytochemical methods, London. Chapman and Hall, Ltd. 1973.pp. 49-188.
[11] ASTM International (ASTM), 100 Barr Harbor Dr., West Conshohocken, PA 19428-2959.
[12] Döner, A, and Kardaş, G. Corrosion Science, 5, 2011, 3(12), 4223-4232.
[13] Bockris, I.O.M. B. Yang, J. Electrochem. Soc. 2012 , 138 2237–2252
[14] Gerengi, H, Sahin, H. I. Industrial & Engineering Chemistry Research, 2011, 51(2), 780- 787.
[15] Satapathy, A.K., Gunasekaran, G, Sahoo, S.C, Kumar Amit, Rodrigues, P.V, Corrosion Science, 2009, 51:2848–2856.
[16] Bentiss, F, Lagrenee, M, Traisnel, M, Hornez, J.C, Corrosion Science, 1999, 41(4): 789-803.
[17] Khamis , E, Hefnawy, A, El-Demerdash, A.M., Material science engineering and technology, 2007, 38(3): 227-232.
[18] McCafferty, E, Hackerman, N. Journal of the Electrochemical Society, 1972,119(2), 146-154.
[19] Havriliak, S, Havriliak, S.J, Dielectric and mechanical relaxation in material analysis, Interpretation and application to polymers, Hanser publisher, Cin-cinnati 1997.
[20] Cruz, J, Pandiyan, T , Ochoa, E.G , Journal of Electroanalytical Chemistry, 2008, 583: 8- 16.
[21] Hassan, H. H, Abdelghani, E , Amin, M. A. Electrochimica Acta, 2007,52(22), 6359- 6366.
[22] Toshima,S , Uchida,T , Electrochimica Acta, 1970,15: 1717-1732.
[23] Leelavathi, S , Rajalakshmi, R , NACE CORROSION 2013, Conference & Expo, NACE International, Orlando, Florida, USA, 17th -21st March 2013.
[24] Fouda, A. S , Tawfik, H , Badr, A. H. Advances in Materials and Corrosion, 2012,1(1), 1-7.
[25] Eddy, N.O , Ebenso, E. E , Ibok. Udo, J ,. Journal of Applied Electrochemistry, 2010, 40: 445-456.
[26] Tebbji, K , Faska, N , Tounsi, A , Oudda, H , Benkaddour, M , Hammouti, B. Materials Chemistry and Physics, 2007, 106(2), 260-267.
[27] Fu, J. J , Li, S. N , Wang, Y , Cao, L. H. Journal of materials science, 2010,45(22), 6255- 6265.
[28] Ivanov, E. S. Inhibitors for metal corrosion in acid media. Metallurgy, Moscow, 1986.
[29] Singh, A.K, Quraishi, M.A, Journal of Materials and Environmental Science, 2010, 1(2): 101-110.

[30] Ekanem, U. F, Umoren, S. A, Udousoro, I. I, Udoh, A. P. Journal of materials science, 2010, 45(20), 5558-5566.
[31] Zerga, B, Attayibat, A, Sfaira, M, Taleb, M, Hammouti, B, Touhami, M. E Rais, Z. Journal of applied electrochemistry, 2010, 40(9), 1575-1582.
[32] Noor, E.A, Journal of Engineering and Applied Sciences, 2008, 3(1): 23-30.
[33] Bentiss,F , Lebrini,M , Lagrenee,M , Corrosion Science, 2005, 47, 2915-2931.
[34] Donahue, F.M., Nobe, K. Theory of organic corrosion inhibitors, Journal of the Electrochemical Society, 1965, 112(9): 886-91.
[35] Ahamad, I, Prasad, R, Quraishi, M.A, Corrosion Science, 2010, 52: 1472.
[36] Moretti, G, Guidi,F, Grion,G , Corrosion Science, 2004, 46: 387–403.
[37] Obi-Egbedi, N.O, Obot, I.B, Arabian Journal of Chemistry, 2010, doi: 10.1016/ j.arabjc .2010.10.004.
[38] Satapathy, A.K, Gunasekaran, G, Sahoo, S.C, Kumar Amit, Rodrigues, P.V, Corrosion Science, 2009, 51:2848–2856.
[39] Ebenso, E.E, Eddy, N.O, Odiongenyi, A.O, African Journal of Pure and Applied Chemistry, 2008, 2(11): 107-115.
[40] Ji, G., Dwivedi, P, Sundaram, S, Prakash, R. Industrial & Engineering Chemistry Research, 2013, 52(31), 10673-10681.
[41] Mourya, P, Banerjee, S, Singh, M. M. Corrosion Science, 2014, 85, 352-363.
[42] Sherif, El-Sayed M, International Journal of Electrochemical science, 2011, 6: 5372 – 5387.
[43] Quraishi, M. A. Industrial & Engineering Chemistry Research, 2014, 53(8), 2851-2859.
[44] Li ,Xianghong , Deng, Shuduan , Fu, Hui , Corrosion Science, 2012, 62: 163–175
[45] Ugbabe, G. E, Ayodele, A. E, Ajoku, G. A, Kunle, O. F, Kolo, I, Okogun, J. I. Glob Res J, 2010, 1, 1-5.
[46] Noor, E. A. International Journal of Electrochemical Science, 2007, 2(12).

Publication History
Received 28th Dec 2015
Revised 20th Jan 2016
Accepted 12th Feb 2016
Online 30th Mar 2016